nature
structural &
molecular biology

Structural basis for autoinhibition of Notch

Wendy R Gordon[1,2], Didem Vardar-Ulu[1–3], Gavin Histen[1], Cheryll Sanchez-Irizarry[1], Jon C Aster[1] & Stephen C Blacklow[1,4]

Notch receptors transmit signals between adjacent cells. Signaling is initiated when ligand binding induces metalloprotease cleavage of Notch within an extracellular negative regulatory region (NRR). We present here the X-ray structure of the human NOTCH2 NRR, which adopts an autoinhibited conformation. Extensive interdomain interactions within the NRR bury the metalloprotease site, showing that a substantial conformational movement is necessary to expose this site during activation by ligand. Leukemia-associated mutations in NOTCH1 probably release autoinhibition by destabilizing the conserved hydrophobic core of the NRR.

© 2007 Nature Publishing Group http://www.nature.com/nsmb

Notch receptors are 300- to 350-kDa type I transmembrane glycoproteins that normally regulate cell growth, differentiation and death in a variety of tissue types[1]. Dysregulation of signaling pathways associated with all four mammalian Notch homologs (Notch1–Notch4) has been implicated in a number of diseases, most notably T-cell acute lymphocytic leukemia[2].

During receptor maturation, the ectodomains of mammalian Notch receptors are cleaved at site S1 by a furin-like protease[3,4], yielding extracellular and transmembrane subunits that are held together by a heterodimerization (HD) domain[5]. Notch activation is normally triggered by the binding of transmembrane ligands of the Delta/Serrate/LAG-2 (DSL) family to the EGF-repeat region of the Notch ectodomain[6,7], which induces a proteolytic cascade called regulated intramembrane proteolysis (RIP). The key proteolytic event that triggers the cascade is a juxtamembrane cleavage by ADAM-type metalloproteases at site S2 (refs. 8,9). S2 cleavage is a necessary prerequisite for a subsequent cleavage by γ-secretase at site S3 (ref. 10), which releases the intracellular part of Notch from the membrane, allowing it to move to the nucleus and regulate gene transcription[11–13] (**Fig. 1a**).

Before ligand-induced activation, Notch is maintained in a resting, metalloprotease-resistant conformation by a conserved NRR, which is sandwiched between the ligand-binding and transmembrane regions of the protein (**Fig. 1a**). The NRR is composed of three Lin12/Notch repeats (LNRs) and the HD domain, which contains the S2 cleavage site. Receptors that lack the EGF repeats are functionally inert[5,11,12,14–16], demonstrating that the restraints on ligand-independent signaling reside in the NRR. Conversely, mutations in the NRRs of Notch receptors produce gain-of-function phenotypes in diverse biological contexts, including developing invertebrates[15,17,18] and patients with T-cell acute lymphoblastic leukemia[2].

To determine how the NRR maintains Notch in a metalloprotease-resistant conformation, gain insight into the mechanism underlying normal ligand-dependent activation of Notch receptors and understand how leukemia-associated mutations circumvent normal restraints on activation, we solved the structure of the human NOTCH2 NRR by X-ray crystallography. The best-diffracting crystals were obtained by removal of 22 residues from an unstructured, poorly conserved loop around the furin cleavage site (**Supplementary Fig. 1** online). The final model, which contains two copies of the NRR in the asymmetric unit, was refined to 2.0-Å resolution (**Supplementary Fig. 2** online) and a final R / R_{free} of 22% / 26%.

RESULTS

Overview of structure

The NRR adopts a compact conformation with overall dimensions of 60 Å × 45 Å × 25 Å (**Fig. 1b**). Numerous interdomain contacts wrap the three LNR modules around the HD domain, bringing the N and C termini of the NRR close together. This arrangement produces a cauliflower-like shape, in which the three LNR module 'florets' cover and protect the HD domain 'stem' (**Fig. 1b**).

Like the prototype LNR from NOTCH1 (ref. 19), the LNR modules share an irregular fold with little secondary structure. Each contains three disulfide bonds with a characteristic connectivity and a bound Ca^{2+} ion coordinated by acidic and polar residues. The first two LNRs (A and B) are connected by a highly conserved, well-ordered 10-residue linker and share a hydrophobic interface formed by the stacking of aromatic residues. In contrast, LNR-C does not make direct contact with either A or B, and the 6-residue linker connecting LNR-B to C is more poorly ordered and not well conserved.

The two halves of the HD domain, normally divided by furin at site S1, form a single protein domain that consists of an intimately

[1]Department of Pathology, Brigham and Women's Hospital and Harvard Medical School, 77 Ave. Louis Pasteur, Boston, Massachusetts 02115, USA. [2]These authors contributed equally to this work. [3]Present address: Department of Chemistry, Wellesley College, 106 Central Street, Wellesley, Massachusetts 02481, USA. [4]Correspondence should be addressed to S.C.B. (sblacklow@rics.bwh.harvard.edu).

Received 29 January; accepted 7 March; published online 1 April 2007; corrected after print 1 April 2007; doi:10.1038/nsmb1227

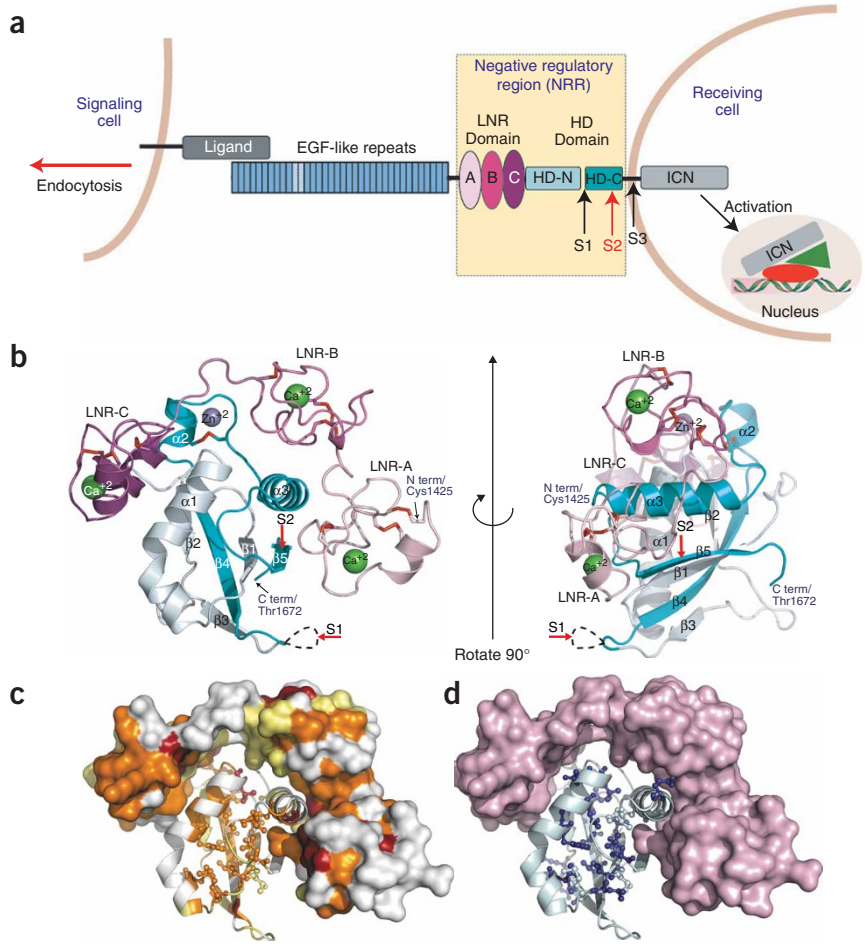

Figure 1 Notch domain organization and overall views of the structure. (**a**) Overview of Notch signaling. Ligand binding to the extracellular portion of Notch triggers metalloprotease cleavage at site S2. The resulting truncated transmembrane subunit of the receptor is a substrate for cleavage at S3 by γ-secretase, which releases the intracellular part of Notch (ICN) from the membrane. ICN migrates to the nucleus, where it assembles into a complex that turns on transcription of target genes. Structure reported here is of the NRR, highlighted in yellow. (**b**) Two views of the NOTCH2 NRR, related by a 90° rotation. Shades of pink and purple, LNR modules; light and dark cyan, HD domain (on N- and C-terminal sides of the furin cleavage loop, respectively); red bonds, disulfide links; red arrows, positions of S1 and S2 cleavage. Bound Ca^{2+} and Zn^{2+} ions are shown. (**c**) NRR structure colored according to sequence conservation (see **Supplementary Fig. 1** for sequence alignment): red, absolutely conserved; orange, highly conserved (Clustal-W strong conservation groups and/or >80% sequence identity); yellow, moderately conserved (Clustal-W weak conservation groups or >50% sequence identity); white, nonconserved. Molecular surface, LNR modules; ribbon, HD domain; ball-and-stick, side chains in hydrophobic core of HD domain, defined as residues in the α/β sandwich having less than 10% solvent accessibility. (**d**) Sites of tumor-associated NOTCH1 HD domain mutations mapped onto the NOTCH2 NRR structure. Pink surface, LNRs; light cyan ribbon, HD domain; ball-and-stick, hydrophobic core residues as in **c**; dark blue, side chains of residues corresponding to tumor-associated mutations.

intertwined α/β sandwich containing five β-strands (β1–β5) and two α-helices (α1 and α3) connected by several conserved loops and a short helix (α2; **Fig. 1b**). The secondary structural elements of the HD fold around a conserved hydrophobic core with side chains that project from residues along the concave surface formed by the β-sheet and from the inner faces of the two flanking helices α1 and α3 (**Fig. 1c**). Notably, almost all of the known leukemia-associated mutations in human NOTCH1 map onto this hydrophobic core, underscoring its importance in maintaining the structural integrity of the HD (**Fig. 1c**,**d**).

Site S1, which was excised from the crystallized construct, would lie in a loop connecting β-strands 3 and 4, more than 17 Å away from the S2 site and well removed from all other interdomain contacts (**Fig. 1**). Site S2 lies near the C-terminal end of the HD domain, in the middle of the final β-strand (β5) and in close proximity to α3. A structural similarity search using the Dali server[20] revealed no significant matches for the LNRs and a single hit for the HD domain with *Z*-score > 6: a 'sea urchin sperm protein, enterokinase and agrin' (SEA) domain (PDB 1IVZ) from murine mucin-16 (ref. 21). Notably, this and homologous mucin SEA domains undergo self-cleavage in the loop connecting strands 2 and 3 of the four-stranded sheet[22], a position that corresponds structurally to the S1 site of the Notch2 HD domain (**Supplementary Fig. 3** online).

Structural basis for autoinhibition

Extensive interactions between the LNR and the HD domains stabilize the NRR in the autoinhibited conformation. The LNRs wrap around the HD domain, masking the S2 site and key structural elements by burying a total solvent-accessible surface area of ~3,000 Å^2 (**Fig. 2a**), almost half of which derives from interactions between LNR C and the HD domain. Hydrophobic residues from LNR-C pack against helices 1 and 2 of the HD domain core, whereas electrostatic interactions between LNR-C and the HD domain fix their relative positions. The charged and polar interactions include a conserved salt bridge between Arg1567 and Asp1506, an extensive hydrogen-bonding network and a Zn^{2+} ion that is coordinated by the side chains of His1574 and His1638 from the HD domain, Glu1525 from LNR-C and a water molecule. Though it is tempting to propose a role for this ion in the regulation of Zn^{2+}-dependent ADAM-metalloproteases, the Zn^{2+}-binding site is not conserved and may simply stabilize the LNR-C–HD domain interface of NOTCH2. A cluster of conserved residues on the exposed surface of LNR-C is a good candidate region for other intra- or intermolecular interactions (**Fig. 1c**).

The remaining long-range interdomain contacts result from the packing of LNR-B, the linker connecting LNR-A and LNR-B (termed LNR-AB linker), and the C-terminal end of LNR-A, which together account for 25%, 23% and 5% of the overall LNR-HD interface, respectively. Together, these interactions mask the S2 site and buttress the HD domain α3 helix (**Fig. 2b**), which is packed against the β-strand housing the S2 site (**Fig. 2c**). The high degree of sequence conservation among the residues engaged in these key intra- and interdomain interactions suggests that the observed autoinhibited conformation is a general feature of Notch receptors (**Fig. 2** and **Supplementary Fig. 1**).

© 2007 Nature Publishing Group http://www.nature.com/nsmb

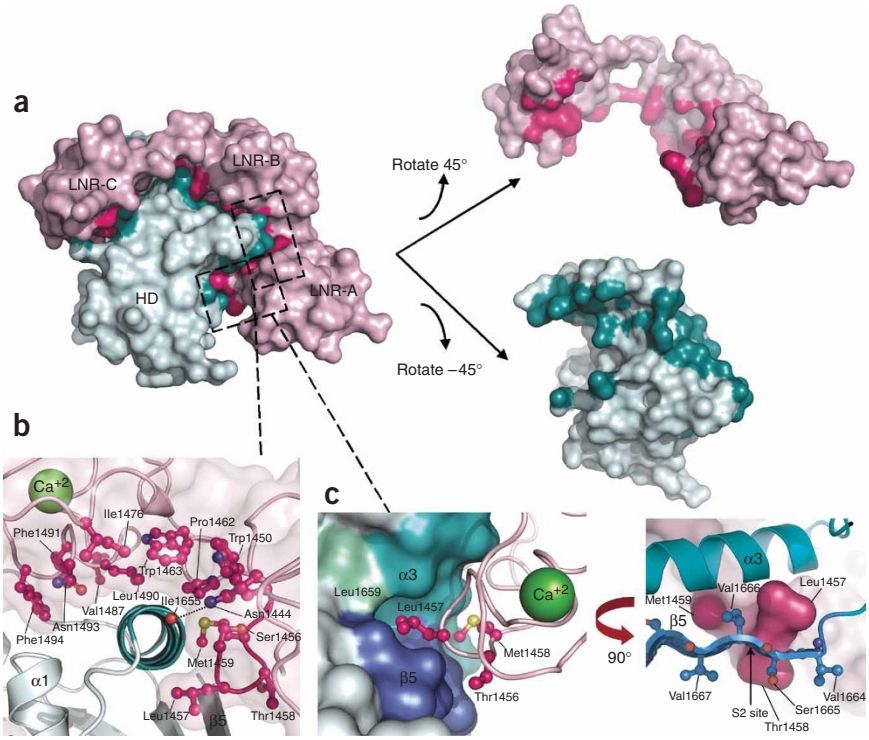

Figure 2 Interface between the LNR and HD domains. (**a**) LNR-HD contact interface. LNR domain surface is colored hot pink when an atom approaches within 4 Å of the HD domain and light pink elsewhere. HD domain is colored teal when an atom approaches within 4 Å of the LNR domain and light cyan elsewhere. (**b**) Anchoring of helix 3. Helix 3 is clamped in position above the S2 site by a hydrophobic interface with residues from LNR-B and the LNR-AB linker and a conserved hydrogen bond from LNR-A. (**c**) The LNR-AB linker sterically blocks access to the metalloprotease cleavage site. Left, hydrophobic pocket in HD domain that houses the S2 site (surface) and residues from the LNR-AB linker (ball-and-stick). Right, view down the scissile bond cleaved by metalloprotease, which has been rotated about 90° from the left view. Residues in β-strand containing the S2 cleavage site are shown as blue ball-and-stick, and three 'gatekeeper residues' from LNR-AB linker as a pink surface.

The S2 site (**Fig. 2c**) is nestled at the mouth of a small hydrophobic pocket bounded by β5 (which contains the Ser1665-Val1666 cleavage site), the inner face of α3 and a highly conserved leucine residue (Leu1659) in the linker that connects these elements. The 'plug' that fills the pocket and blocks access to the scissile bond is the side chain of Leu1457, which lies in the linker connecting LNR-A and B (**Fig. 2c**). Leu1457 is fixed in the pocket by a hydrogen bond between its carbonyl oxygen and the backbone amide of Val1666 and by packing against residues that line the pocket (Leu1650, Ala1651, Ala1654, Leu1663 and Val1666), which account for 10% of the total LNR-HD domain interface. Together, the side chains of Leu1457, Thr1458 and Met1459 straddle the S2 site and prevent access from either side (**Fig. 2c**). Precise anchoring of HD domain helix 3 above the S2 site also maintains the pocket. This helix is clamped into position by hydrophobic residues derived from the LNR-AB linker (Met1459, Pro1462 and Trp1463) and LNR-B (Ile1476, Val1487, Leu1490, Asn1493 and Phe1494; see **Fig. 2b**). In addition, a hydrogen bond between the Asn1444 side chain of LNR-A and the backbone carbonyl group of Ile1655 anchors helix 3 at its C-terminal end. The burial of the S2 site establishes the need for a substantial conformational movement to enable metalloprotease cleavage in response to ligand binding.

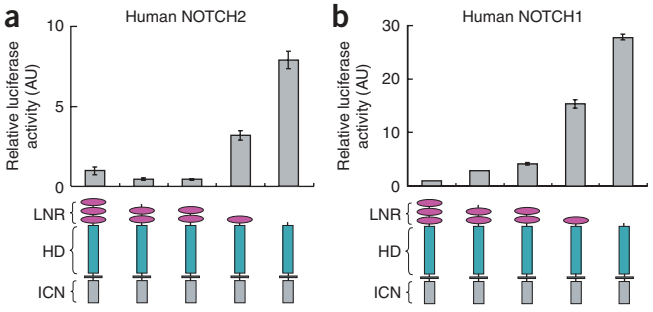

Figure 3 Cell-based reporter gene assays showing that stepwise removal of LNR domain elements causes ligand-independent activation of NOTCH. (**a**,**b**) Luciferase assays were done in triplicate on U2OS cell lysates prepared from cells transfected with 10 ng of plasmids encoding the NOTCH2-NOTCH1 chimeric constructs shown schematically below graph (**a**; see Methods) or NOTCH1 (**b**), along with a luciferase reporter plasmid containing iterated CSL-binding sites and an internal control plasmid expressing *Renilla* luciferase. Firefly luciferase activity from cell lysates was measured in triplicate, normalized and plotted relative to the activity in extracts prepared from cells transfected with the ΔEGF NOTCH2-NOTCH1 chimera (**a**) or ΔEGF NOTCH1 (**b**). AU, arbitrary units. Error bars represent s.d.

Effect of interdomain interactions on Notch function

To begin to address the functional importance of the autoinhibitory interdomain interactions, we used the structure to guide the design of nested NOTCH1 and NOTCH2 NRR deletions and determined the effects of the deletions on receptor activation in cells (**Fig. 3**). These experiments show that LNR-A, the LNR-AB linker and LNR-B must all be removed before activation occurs, consistent with the structural prediction that key interactions of LNR-B and the LNR-AB linker with the HD domain protect the metalloprotease site.

DISCUSSION

The mechanism by which ligand binding triggers S2 cleavage to activate Notch signaling has remained elusive. Models have been proposed in which the S2 site is exposed by ligand-induced conformational changes, changes in the oligomeric state of the receptor or dissociation of the HD subunits[23]. Genetic and functional studies showing that endocytosis of Notch ligands on signaling cells is crucial for Notch activation[24–33] have led to a number of mechanistic proposals to account for this requirement, including the following. (i) Binding of the Notch extracellular subunit to ligand causes mechanical strain that induces a conformational change to expose the S2 site[34]. (ii) Endocytosis of Notch-bound ligand dissociates partner proteins (either Notch oligomers interacting in *cis* or other polypeptides) that mask S2 (ref. 34). (iii) Endocytosis and ligand recycling enable clustering[1], relocalization[25] or a post-translational

© 2007 Nature Publishing Group http://www.nature.com/nsmb

modification of ligand that is needed for Notch activation[26]. These latter possibilities are not mutually exclusive with other proposed roles for endocytosis.

Our structure provides the first direct experimental evidence that a substantial conformational movement in the NRR is required to expose the S2 site upon ligand binding and strongly opposes models that require changes in oligomerization or other intermolecular interactions to uncover the S2 site. In addition, the subunits comprising the HD domain are woven into an intimately intertwined α/β sandwich by an extensive hydrogen-bonding network, which disfavors models in which ligand binding causes the dissociation of the subunits to expose S2 without first disengaging the LNR domain from the HD domain.

The structure of the autoinhibited conformation does not itself show whether ligand binding causes a simple allosteric conformational change in the NRR or whether endocytosis of ligand bound to Notch is required to exert a mechanical force to activate the receptor, as previously proposed[34]. In the mechanical-force model for activation, which we refer to as the 'lift-and-cut' model, force would induce the conformational movement that renders Notch susceptible to S2 cleavage by peeling the protective LNR modules away from the HD domain. As the ligand-binding domain is immediately adjacent to LNR-A of the NRR on the N-terminal side, the mechanical tug would first lift LNR-A, then LNR-B and finally LNR-C away from the HD domain. Effective transmission of force to the NRR would require a tight interaction between ligand and receptor, which is supported by direct measurements of adhesion strength in pairs of cells expressing Notch and ligand, respectively[35], and by prior observations of Notch ectodomain *trans*-endocytosis into ligand-bearing cells[34]. The extent of the proposed movement is consistent with prior studies showing that the active site of TNFα-converting enzyme (TACE), a metalloprotease implicated in S2 cleavage of Notch, is buried in a hydrophobic groove that cups the substrate from both sides of the scissile bond[36]. As a result, it appears that both the hydrophobic plug that fills the pocket containing the scissile bond and the interdomain interactions that clamp helix 3 in the HD must be disrupted for TACE to access the S2 site.

Alternatively, ligand binding could induce conformational exposure of the S2 site allosterically, without exerting a pulling force on the receptor. Because the interface between the LNR and HD domains is extensive (burying ~3,000 Å^2), it seems less likely that binding of ligand to the EGF-repeat region almost 1,000 residues away from the S2 site can provide the required energy to disrupt this interface by an allosteric mechanism. However, even though engineered soluble ligands act as antagonists in vertebrates and flies[37,38], worms do produce a natural secreted ligand that activates Notch[39]. This observation suggests either that worms have evolved an adaptor molecule that stably tethers the secreted ligand to allow for the development of force or that ligands can indeed induce exposure of the metalloprotease site by an allosteric, rather than force-dependent, mechanism.

The structure reported here provides a concrete basis for further experiments to distinguish between the mechanical-force and allosteric models for activation of Notch. If force is responsible for normal receptor activation, it will then be of interest to determine the magnitude of force necessary to release autoinhibition, as well as the stoichiometry of ligand–Notch complexes necessary to transduce such a force. In addition, if mechanotransduction triggers RIP in Notch, then it may also have a role in the cleavage of other transmembrane proteins that undergo RIP, such as the amyloid precursor protein.

The mechanism for autoinhibition proposed here for human NOTCH2 is likely to be general for all Notch receptors, given their high degree of homology. However, sequence differences among the four mammalian Notch receptors and across species also suggest subtle, but potentially important, differences. Most notably, the length and composition of the linker connecting the ligand-binding EGF repeats to the NRR is highly divergent among the four mammalian Notch receptors, suggesting that the responses of these four receptors to ligand may vary. The precise molecular basis for protection of the S2 site in the autoinhibited state may also differ in some Notch receptors. In *Caenorhabditis elegans* lin12, for example, the highly conserved Leu1457 plug that masks the S2 site in the NRR of NOTCH2 is replaced by an arginine residue that probably forms a protective salt bridge with a glutamate residue near its presumed S2 site on β5. This alternative protective mechanism is in line with prior identification of gain-of-function mutations involving these two residues[18].

Our structure of the NRR also provides insight into the ligand-independent activation of NOTCH1 caused by leukemia-associated HD domain mutations[2,40]. The most common mutations lie within the hydrophobic core of the HD (**Fig. 1c,d**) and cause increased sensitivity to S2 cleavage and decreased NRR stability[40]. These hydrophilic and nonconservative amino acid substitutions within the hydrophobic core of the HD domain probably act by partially or completely unfolding the domain, thereby destroying the small hydrophobic pocket that houses the S2 site and preventing the LNRs from protecting it (**Fig. 1d**). This possibility is supported by biochemical data showing that mutations of this class destabilize the S1-cleaved HD domain of NOTCH1 (ref. 40). A second, less frequent group of mutations, which consist of insertions of 12–14 residues immediately adjacent to the S2 site on the N-terminal side, probably displace the NRR and leave the S2 site unprotected[40]. The autoinhibited conformation reported here opens a new avenue for the development of therapeutics that target Notch signaling, enabling a structure-based search for small molecules or antibodies designed to either stabilize (for example, as a treatment of T-cell acute lymphocytic leukemia) or disrupt the restrained conformation of the receptor.

METHODS

Protein expression and purification. The NRR from human NOTCH2 (SWISS-PROT accession code Q04721, residues 1423–1677) was subcloned into a pET 15b vector containing a hexahistidine tag and a custom tobacco etch virus (TEV) site. The crystallized protein has 22 residues removed from the nonconserved, unstructured loop (residues 1595–1616) containing the furin cleavage site, and it also contains an additional glycine at the N terminus resulting from TEV cleavage to release the tag. The protein was produced recombinantly in Rosetta(DE3)pLysS bacteria and recovered from the insoluble fraction after centrifugation using 5 M urea. The protein was affinity-purified on a nickel column, eluted with imidazole in 1 M urea and treated with TEV protease to remove the His tag. The protein was refolded *in vitro* by dialysis in a redox buffer containing 5 mM cysteine and 1 mM cystine, and purified by anion-exchange chromatography after folding was complete (as monitored by reverse-phase HPLC) to obtain a homogenous species. Selenomethionine (SeMet) was incorporated into the protein using standard methods (**Table 1**).

Crystallization. Native NOTCH2 NRR crystallized in 100 mM Bis-Tris (pH 6.5), 200 mM $MgCl_2$, 18% (w/v) PEG 3,350 and 10% (v/v) glycerol at pH 6.5. SeMet-labeled protein crystallized in 100 mM Tris (pH 8.5), 200 mM $MgCl_2$, 24% (w/v) PEG 3,350 and 10% (v/v) glycerol. Crystals were frozen in the same solutions, except with a concentration of PEG 3,350 greater by 2% (w/v) and a final glycerol concentration of 20% (v/v).

Data collection and scaling. Data was collected at beamline X29A at the National Synchrotron Light Source of Brookhaven National Laboratory using

© 2007 Nature Publishing Group http://www.nature.com/nsmb

Table 1 Data collection, phasing and refinement statistics

	Human NOTCH2 NRR
Data collection	
Space group	$P2_12_12_1$
Cell dimensions	
a, *b*, *c* (Å)	45.4, 74.7, 139.4
Resolution (Å)	30.0–2.0 (2.07–2.0)
R_{merge}	7.5 (40.5)
$I / \sigma I$	17.2 (3.2)
Completeness (%)	97.2 (98.1)
Redundancy	4.9 (4.7)
Refinement	
Resolution (Å)	30.0–2.0
No. reflections	31,732
R_{work} / R_{free}	22.4 / 26.8
No. atoms	
Protein	3,411
Ions	7
Water, glycerol	183, 10
B-factors	
Protein	
(molecule 1 in ASU)	43
(molecule 2 in ASU)	54
Ions	57
Water	58
R.m.s. deviations	
Bond lengths (Å)	0.01
Bond angles (°)	1.174

Highest-resolution shell is shown in parentheses. ASU, asymmetric unit.

the Crystallography at Brookhaven Acquisition Software System (CBASS). HKL2000 (ref. 41) was used for indexing and scaling.

Phasing. Phases were calculated by multiple isomorphous replacement with anomalous scattering using auto-Sharp (Global Phasing). Data collected at the peak wavelength (0.979 Å) for four SeMet-labeled crystals and one native crystal were used as input for phasing. The experimentally phased electron density map allowed automated building of approximately half of the model by ARP/wARP[42] (in the auto-Sharp interface).

Refinement. The NOTCH2 NRR model contained two copies of the NRR in the asymmetric unit. The noncrystallographic symmetry (NCS) between these two molecules was used to calculate NCS-averaged maps (Rave, Uppsalla group) to aid in manual building. NCS restraints were relaxed during iterative manual building in COOT[43] and refinement with CNS[44] and REFMAC[45]. The final model contains 183 molecules of solvent and 10 of glycerol, with an overall R_{cryst} / R_{free} of 22.4% / 26.8% at 2.0-Å resolution. The percentages of protein residues in core, allowed, generous and disallowed regions of the Ramachandran plot are 81.3, 16.3, 2.5 and 0.0, respectively.

Constructs used in cell-based reporter assays. All Notch expression plasmids were engineered to contain the start codon and the signal peptide of NOTCH1 in the mammalian expression vector pcDNA3.1. NOTCH2-NOTCH1 chimeras were made by ligation of PCR products amplified from a NOTCH2 complementary DNA into the NOTCH1 ΔEGF cDNA after digestion with the restriction enzymes BamHI and Bsu36I. The resulting chimeric cDNAs encoded polypeptides comprised of the NOTCH1 leader peptide, portions of the ectodomain of NOTCH2, the transmembrane domain of NOTCH2 and the first 13 amino acid residues of the intracellular domain of NOTCH2 fused to all but the first 13 amino acid residues of the intracellular domain of NOTCH1. The ΔEGF NOTCH2-NOTCH1 chimera starts with residue Pro1422 of NOTCH2. Constructs with further deletions start with NOTCH2 residue Ser1456 (ΔEGFΔLNR-A), Pro1462 (ΔEGFΔLNR-AΔlink), Gln1497 (ΔEGFΔLNR-AB) or Ala1535 (ΔEGFΔLNR-ABC). The ΔEGF form of NOTCH1 begins with residue Glu1446 of NOTCH1, after the BamHI site that follows the signal peptide[5]. Constructs with further deletions start with Ser1481 (ΔEGFΔLNR-A), Lys1489 (ΔEGFΔLNR-AΔlink), Gln1523 (ΔEGFΔLNR-AB) or His1564 (ΔEGFΔLNR-ABC).

Accession codes. Protein Data Bank: Coordinates have been deposited with accession code 2OO4.

Note: Supplementary information is available on the Nature Structural & Molecular Biology website.

ACKNOWLEDGMENTS

We thank Mike Eck and Angela Toms for crystallographic suggestions and Kelly Arnett and Mike Malecki for critical reading of the manuscript. This work was supported by American Cancer Society Postdoctoral Fellowships (WRG and DVU), a Leukemia and Lymphoma Society Fellowship (WRG), and NIH grants to SCB and JCA.

COMPETING INTERESTS STATEMENT

The authors declare no competing financial interests.

Published online at http://www.nature.com/nsmb
Reprints and permissions information is available online at http://npg.nature.com/reprintsandpermissions

1. Bray, S.J. Notch signalling: a simple pathway becomes complex. *Nat. Rev. Mol. Cell Biol.* **7**, 678–689 (2006).
2. Weng, A.P. *et al.* Activating mutations of NOTCH1 in human T cell acute lymphoblastic leukemia. *Science* **306**, 269–271 (2004).
3. Blaumueller, C.M., Qi, H., Zagouras, P. & Artavanis-Tsakonas, S. Intracellular cleavage of Notch leads to a heterodimeric receptor on the plasma membrane. *Cell* **90**, 281–291 (1997).
4. Logeat, F. *et al.* The Notch1 receptor is cleaved constitutively by a furin-like convertase. *Proc. Natl. Acad. Sci. USA* **95**, 8108–8112 (1998).
5. Sanchez-Irizarry, C. *et al.* Notch subunit heterodimerization and prevention of ligand-independent proteolytic activation depend, respectively, on a novel domain and the LNR repeats. *Mol. Cell. Biol.* **24**, 9265–9273 (2004).
6. Fehon, R.G. *et al.* Molecular interactions between the protein products of the neurogenic loci Notch and Delta, two EGF-homologous genes in *Drosophila*. *Cell* **61**, 523–534 (1990).
7. Weinmaster, G. The ins and outs of notch signaling. *Mol. Cell. Neurosci.* **9**, 91–102 (1997).
8. Brou, C. *et al.* A novel proteolytic cleavage involved in Notch signaling: the role of the disintegrin-metalloprotease TACE. *Mol. Cell* **5**, 207–216 (2000).
9. Mumm, J.S. *et al.* A ligand-induced extracellular cleavage regulates gamma-secretase-like proteolytic activation of Notch1. *Mol. Cell* **5**, 197–206 (2000).
10. Kopan, R. & Goate, A. A common enzyme connects notch signaling and Alzheimer's disease. *Genes Dev.* **14**, 2799–2806 (2000).
11. Schroeter, E.H., Kisslinger, J.A. & Kopan, R. Notch-1 signalling requires ligand-induced proteolytic release of intracellular domain. *Nature* **393**, 382–386 (1998).
12. Struhl, G. & Adachi, A. Nuclear access and action of notch *in vivo*. *Cell* **93**, 649–660 (1998).
13. Struhl, G., Fitzgerald, K. & Greenwald, I. Intrinsic activity of the Lin-12 and Notch intracellular domains *in vivo*. *Cell* **74**, 331–345 (1993).
14. Kopan, R., Schroeter, E.H., Weintraub, H. & Nye, J.S. Signal transduction by activated mNotch: importance of proteolytic processing and its regulation by the extracellular domain. *Proc. Natl. Acad. Sci. USA* **93**, 1683–1688 (1996).
15. Lieber, T., Kidd, S., Alcamo, E., Corbin, V. & Young, M.W. Antineurogenic phenotypes induced by truncated Notch proteins indicate a role in signal transduction and may point to a novel function for Notch in nuclei. *Genes Dev.* **7**, 1949–1965 (1993).
16. Rebay, I., Fehon, R.G. & Artavanis-Tsakonas, S. Specific truncations of *Drosophila* Notch define dominant activated and dominant negative forms of the receptor. *Cell* **74**, 319–329 (1993).
17. Berry, L.W., Westlund, B. & Schedl, T. Germ-line tumor formation caused by activation of glp-1, a *Caenorhabditis elegans* member of the Notch family of receptors. *Development* **124**, 925–936 (1997).
18. Greenwald, I. & Seydoux, G. Analysis of gain-of-function mutations of the *lin-12* gene of *Caenorhabditis elegans*. *Nature* **346**, 197–199 (1990).
19. Vardar, D., North, C.L., Sanchez-Irizarry, C., Aster, J.C. & Blacklow, S.C. Nuclear magnetic resonance structure of a prototype Lin12-Notch repeat module from human Notch1. *Biochemistry* **42**, 7061–7067 (2003).
20. Holm, L. & Sander, C. Mapping the protein universe. *Science* **273**, 595–603 (1996).
21. Maeda, T. *et al.* Solution structure of the SEA Domain from the murine homologue of ovarian cancer antigen CA125 (MUC16). *J. Biol. Chem.* **279**, 13174–13182 (2004).
22. Macao, B., Johansson, D.G.A., Hansson, G.C. & Hard, T. Autoproteolysis coupled to protein folding in the SEA domain of the membrane-bound MUC1 mucin. *Nat. Struct. Mol. Biol.* **13**, 71–76 (2006).

© 2007 Nature Publishing Group http://www.nature.com/nsmb

23. Mumm, J.S. & Kopan, R. Notch signaling: from the outside in. *Dev. Biol.* **228**, 151–165 (2000).
24. Itoh, M. *et al.* Mind bomb is a ubiquitin ligase that is essential for efficient activation of Notch signaling by Delta. *Dev. Cell* **4**, 67–82 (2003).
25. Le Borgne, R., Bardin, A. & Schweisguth, F. The roles of receptor and ligand endocytosis in regulating Notch signaling. *Development* **132**, 1751–1762 (2005).
26. Wang, W. & Struhl, G. *Drosophila* Epsin mediates a select endocytic pathway that DSL ligands must enter to activate Notch. *Development* **131**, 5367–5380 (2004).
27. Wang, W. & Struhl, G. Distinct roles for Mind bomb, Neuralized and Epsin in mediating DSL endocytosis and signaling in *Drosophila*. *Development* **132**, 2883–2894 (2005).
28. Bingham, S. *et al.* Neurogenic phenotype of mind bomb mutants leads to severe patterning defects in the zebrafish hindbrain. *Dev. Dyn.* **228**, 451–463 (2003).
29. Lai, E.C., Roegiers, F., Qin, X., Jan, Y.N. & Rubin, G.M. The ubiquitin ligase *Drosophila* Mind bomb promotes Notch signaling by regulating the localization and activity of Serrate and Delta. *Development* **132**, 2319–2332 (2005).
30. Le Borgne, R., Remaud, S., Hamel, S. & Schweisguth, F. Two distinct E3 ubiquitin ligases have complementary functions in the regulation of delta and serrate signaling in *Drosophila*. *PLoS Biol.* **3**, 688–696 (2005).
31. Le Borgne, R. & Schweisguth, F. Unequal segregation of Neuralized biases Notch activation during asymmetric cell division. *Dev. Cell* **5**, 139–148 (2003).
32. Pavlopoulos, E. *et al.* neuralized encodes a peripheral membrane protein involved in delta signaling and endocytosis. *Dev. Cell* **1**, 807–816 (2001).
33. Seugnet, L., Simpson, P. & Haenlin, M. Requirement for dynamin during Notch signaling in *Drosophila* neurogenesis. *Dev. Biol.* **192**, 585–598 (1997).
34. Parks, A.L., Klueg, K.M., Stout, J.R. & Muskavitch, M.A. Ligand endocytosis drives receptor dissociation and activation in the Notch pathway. *Development* **127**, 1373–1385 (2000).
35. Ahimou, F., Mok, L.P., Bardot, B. & Wesley, C. The adhesion force of Notch with Delta and the rate of Notch signaling. *J. Cell Biol.* **167**, 1217–1229 (2004).
36. Maskos, K. *et al.* Crystal structure of the catalytic domain of human tumor necrosis factor-alpha-converting enzyme. *Proc. Natl. Acad. Sci. USA* **95**, 3408–3412 (1998).
37. Sun, X. & Artavanis-Tsakonas, S. Secreted forms of DELTA and SERRATE define antagonists of Notch signaling in Drosophila. *Development* **124**, 3439–3448 (1997).
38. Varnum-Finney, B. *et al.* Immobilization of Notch ligand, Delta-1, is required for induction of notch signaling. *J. Cell Sci.* **113**, 4313–4318 (2000).
39. Chen, N. & Greenwald, I. The lateral signal for LIN-12/Notch in *C. elegans* vulval development comprises redundant secreted and transmembrane DSL proteins. *Dev. Cell.* **6**, 183–192 (2004).
40. Malecki, M.J. *et al.* Leukemia-associated mutations within the NOTCH1 heterodimerization domain fall into at least two distinct mechanistic classes. *Mol. Cell. Biol.* **26**, 4642–4651 (2006).
41. Otwinowsk, Z. & Minor, W. Processing of X-ray diffraction data collected in oscillation mode. *Methods Enzymol.* **276**, 307–326 (1997).
42. Perrakis, A., Morris, R. & Lazmin, V. Automated protein model building combined with iterative structure refinement. *Nat. Struct. Biol.* **6**, 458–463 (1999).
43. Emsley, P. & Cowtan, K. Coot: model-building tools for molecular graphics. *Acta Crystallogr. D Biol. Crystallogr.* **60**, 2126–2132 (2004).
44. Brunger, A.T., Adams, P. & Clore, G. Crystallography and NMR system: a new software suite for macromolecular structure determination. *Acta Crystallogr D Biol. Crystallogr.* **54**, 905–921 (1998).
45. Murshudov, G., Vagin, A. & Dodson, E. Refinement of macromolecular structures by the maximum-likelihood method. *Acta Crystallogr. D Biol. Crystallogr.* **53**, 240–245 (1997).

© 2007 Nature Publishing Group http://www.nature.com/nsmb